

ESTIMATION OF EQUIVALENT VISCOUS DAMPING RATIO FOR FLEXURAL BEAM IN PRESTRESSED REINFORCED CONCRETE FRAME



Tajima Yuji

Asiss Corporation, Japan

Kitayama Kazuhiro

Tokyo Metropolitan University, Japan

SUMMARY:

This paper focuses on quantitative estimation of an equivalent viscous damping ratio (denoted as h_{eq}) for a flexural beam in a prestressed reinforced concrete (called as PRC) building. An available expression for a design practice to estimate the h_{eq} for a flexural beam within PRC interior beam-column subassemblages is proposed empirically using previous test results for cruciform beam-column subassemblage specimens. Energy dissipating ability in a PRC flexural beam is dominated by a contribution ratio of a tensile force in a PC tendon to an ultimate flexural capacity of a beam critical section, and both bond situation along a beam bar and a PC tendon passing through a beam-column joint panel. Thus these factors are taken into account in a proposed equation. An equivalent viscous damping ratio predicted by the equation for a PRC flexural beam within interior beam-column subassemblages agreed well with that obtained by laboratory tests.

Keywords: Prestressed Reinforced Concrete, Equivalent Viscous Damping Ratio, Bond along PC Tendon

1. INTRODUCTION

1.1. Objectives

Prestressed concrete (called as PC) structures have still been designed by the ultimate strength design method since "Standard for Structural Design and Construction of Prestressed Concrete Structures" was published by the Architectural Institute of Japan in 1961. In contrast, a research for a reinforced concrete (called as RC) structure has been advanced to develop the performance-based design method. However, for a PC structure, the performance-based design method is not established. Some hysteretic characteristic models for a flexural PC beam were proposed using past test results under static cyclic load reversals. In order to predict nonlinear seismic response for PC buildings with a sufficient accuracy using these models, an equivalent viscous damping ratio h_{eq} which indicates energy dissipation performance for a PC beam is needed to predict hysteresis behaviour for the beam. Then it is very useful to estimate the performance of the energy dissipation.

Therefore, this paper focuses on quantitative estimation of the h_{eq} for a flexural beam in a PRC building. An available expression to estimate the h_{eq} for a flexural beam within PRC interior beam-column subassemblages is proposed empirically using previous test results for cruciform beam-column subassemblage specimens in references [Kishida S.] and [Kitayama K.].

1.2. Past Studies (Referred Equation)

The equation (1.1) to estimate the h_{eq} for a flexural beam in a RC building has been proposed in reference [Architectural Institute of Japan]. A bond index B_f for a beam bar within a beam-column joint panel is taken into account in the equation (1.1);

$$h_{eq} = 0.09 + \frac{0.1}{B_f^2} \cdot \left(1 - \frac{1}{\sqrt{\mu}} \right) \quad (1.1)$$

where μ : ductility factor for a deformation in a force-deformation relation of a beam.

The bond index B_I indicates a bond condition along a beam bar within a RC joint panel, which is expressed as follows;

$$B_I = \frac{u_{b,av}}{\tau_u} \quad (1.2)$$

where the $u_{b,av}$ indicates an average bond stress along beam bars passing through a RC joint panel when beam bars have tensile yield stress at a beam critical section and have compressive stress computed from force equilibrium at the opposite beam critical section. This bond stress $u_{b,av}$ is expressed as follows;

$$u_{b,av} = \frac{3 + \gamma}{8} \frac{\sigma_y \cdot d_b}{D_c} \quad (1.3)$$

where γ : ratio of a sectional area for tensile reinforcement to compressive reinforcement at a beam section, σ_y : yield strength of a beam bar, d_b : a diameter of a beam bar and D_c : column depth.

The τ_u indicates the bond strength along a beam bar passing through a RC joint panel, which is expressed as follows;

$$\tau_u = 0.7 \left(1 + \frac{\sigma_0}{\sigma_B} \right) \sigma_B^{2/3} \quad (1.4)$$

where σ_0 : column axial stress and σ_B : concrete compressive strength.

2. PREVIOUS TEST PROGRAM

2.1. Specimens

Properties and failure modes of specimens are summarized in Table 2.1. Material properties of steel and PC tendon are listed in Table 2.2. The surface shapes of used sheath tubes and PC tendons are shown in Figure 2.1 and 2.2, respectively. Section dimensions and reinforcement details are shown in Figure 2.3. All specimens were fabricated with two-fifth scale. The column section was square with 350mm depth and width. The depth and width of the beam section were 400mm and 250mm, respectively. The length from a center of the column to the support of a beam end was 1600mm. The height from a center of the beam to the loading point on the top of the column or to the bottom support was 1415mm, respectively. The shear span ratio was 3.5 for the column and 3.7 for the beam.

Two types of failure mode were observed in the tests. One was caused by rupture or buckling of a beam longitudinal bar after yielding of both longitudinal bars and PC tendons, denoted by BY in Table 2.1. Another was caused by concrete crushing at the beam end without yielding of PC tendons, denoted by B in Table 2.1. Only specimen BNN2 failed in concrete compression at the beam end after PC tendons yielded. Concrete compressive strength was 59 to 77MPa. Grout compressive strength was 54 to 65MPa. Except for Specimen BNN2 the effective post-tensioning force equal to the stress about 0.54 times the yield strength of the PC tendon was provided. For Specimen BNN2 the effective post-tensioning force equal to the stress about 0.29 times the yield strength of the PC tendon was provided. A contribution ratio of PC tendons to ultimate flexural capacity of a PRC beam section, called the prestressing ratio (denoted as λ) in the paper, ranged from 0.36 to 1.00. The bond along post-tensioning steel bars was provided by injecting grout mortar into a sheath tube.

2.2. Loading Method and Instrumentation

A loading apparatus is shown in Figure 2.4 and Photograph 2.1. The beam ends were supported by horizontal rollers, while the bottom of the column was supported by a universal joint. The reversed lateral horizontal loads and the constant axial load in compression (an axial load ratio of 0.10~0.13) were applied at the top of the column through a tri-directional joint by three oil jacks. In this paper a story drift angle is expressed as a percent ratio of a lateral displacement at the tri-directional joint to the column height 2830mm. Specimens N-4, N-5, M-2, M-5, UB-1, GB-2, SB-3 and GBS-4 were controlled by a story drift angle for one loading cycle of 0.25 %, two cycles of 0.5 %, three cycles of 1 %, 1.5%, 2 %, 3 % and 4 % respectively, and one-way loading to 5 %. Specimens BNN2, WNN, and BNU were controlled by a story drift angle for one loading cycle of 0.25 %, two cycles of 0.5 %, and one-way loading to 5 %.

Table 2.1 Properties of specimens

Specimen	N-4 ^[2]	N-5 ^[2]	M-2 ^[2]	M-5 ^[2]	UB-1 ^[3]	GB-2 ^[3]	SB-3 ^[3]	GBS-4 ^[3]	BNN2 ^[1]	WNN ^[1]	BNU ^[1]
Concrete compressive strength	63.4 (MPa)		58.8 (MPa)		77.2 (MPa)			76.1 (MPa)			
Grout compressive strength	56.4 (MPa)				65.3 (MPa)			54.0 (MPa)			
Beam PC tendon	4-φ10.7		2-φ9.2	2-φ12.6	2-D22	2-D22	2-D22	3-φ12.6	2-D32	5-12.4A	2-D32
Surface shape of PC tendon	Fig. 2.1(a)				Fig. 2.1(b)			Fig.2.1(a)	Fig.2.1(b)	Fig.2.1(c)	Fig.2.1(b)
Effective prestressing stress/Yield strength	0.55	0.50	0.61	0.54	0.53	0.51	0.51	0.51	0.29	0.56	0.57
Top beam longitudinal bars	4-D13	2-D13	3-D13	2-D19	2-D13	2-D13	2-D13	3-D13	/		
Japanese Industrial Standards	SD345	SD295A	SD345	SD345	SD295A	SD295A	SD295A	SD490			
Bottom beam longitudinal bars	2-D19	2-D13	3-D13	2-D19	2-D13	2-D13	2-D13	3-D13			
Japanese Industrial Standards	SD345	SD295A	SD345	SD345	SD295A	SD295A	SD295A	SD490			
Prestressing ratio (λ) ^{*1}	0.51	0.71	0.36	0.43	0.74	0.80	0.80	0.69	1.00		
Sheath tube	#1026			#1028	#1040		#3040	#1028	#1049	#1056	#1049
Column longitudinal bars	12-D22(SD345)								4-D32(SBPR 930/1080)		
Beam stirrup	2-D13@100								2-D10@100		
Column hoop	2-D10@100								2-D10@100		
Column axial load	930 (kN)										
Failure type	BY	BY	BY	BY	B	BY	BY	BY	B	B	B
Beam section											

*1: Prestressing ratio λ is a contribution ratio of PC tendons to ultimate flexural capacity of a PRC beam

Table 2.2 Material properties of steel bars

	Diameter	Japanese Industrial Standards	Yield strength	Nominal Young's modulus	Yield strain	Tensile strength	Elastic limit strain
			MPa	GPa	%	MPa	%
Deformed bar	D10	SD345	400	184	0.22	552	/
	D10	SD390	444	199	0.22	635	
	D13	SD295A	356	175	0.20	494	
	D13	SD345	376	180	0.21	547	
	D13	SD490	564	186	0.30	717	
	D13	USD685A	724	190	0.42	937	
	D19	SD345	380	182	0.21	574	
	D22	SD345	373	186	0.20	503	
PC tendon	φ9.2	SBPDN	1375	186	0.95	1456	0.66
Deformed bar with twisted	φ10.7	SBPDN	1350	199	0.91	1450	0.59
	φ12.6	SBPDN	1420	195	0.92	1471	0.60
PC tendon	D22	SBPR	1042	200	0.73	1166	0.46
Deformed bar	D32	SBPR	1014	195	0.72	1164	0.33
PC tendon	12.4A	SWPR7A	1795	220	1.02	1901	0.36

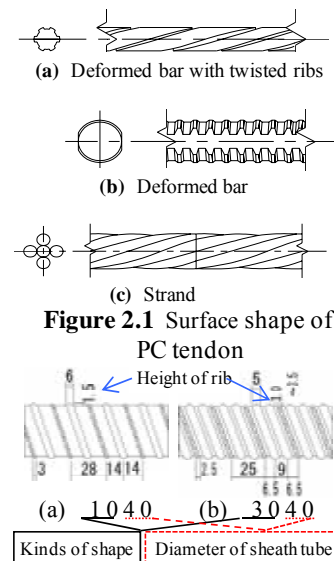


Figure 2.2 Shape of sheath tube

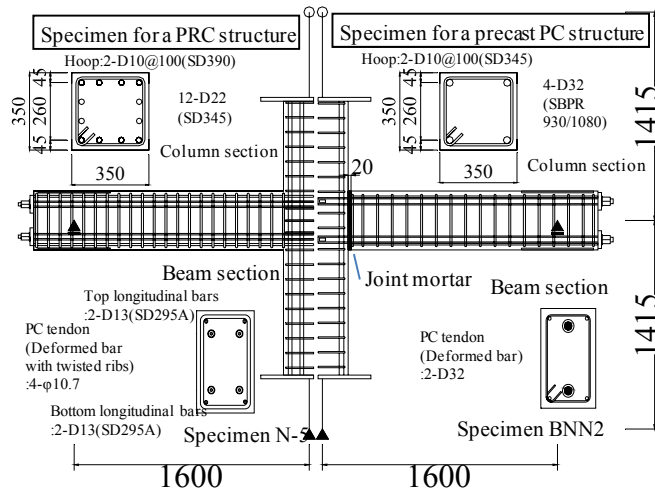


Figure 2.3 Section dimensions and reinforcement details

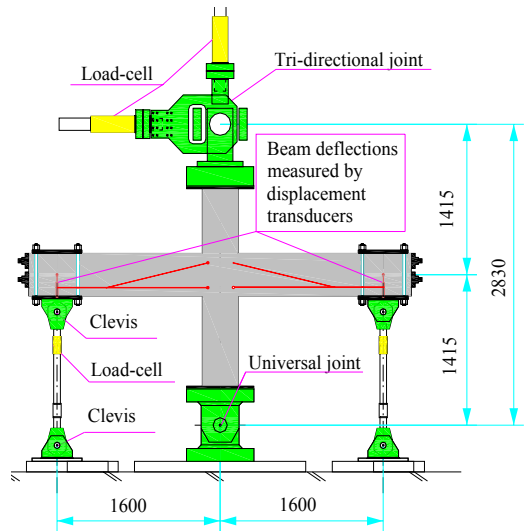


Figure 2.4 Loading apparatus

1 %, 1.5% and 2 % respectively, one cycle of 3 %, two cycles of 4 % and one-way loading to 5 %. Lateral forces, column axial load and beam shear forces were measured by load-cells. Story drift, beam and column deflections, and local displacement of a joint panel were measured by displacement transducers. Strains of prestressing steel bars, beam bars, column bars and joint lateral reinforcement were measured by strain gauges. Concrete normal strain at a beam end adjacent to a column face was measured by strain gauges attached on concrete surface.

3. TEST RESULTS AND DISCUSSIONS

3.1. Beam Shear – Deflection Relations

Beam shear force-beam deflection angle (denoted as R_b) relations are shown in Figure 3.1 in order of λ . In this paper a R_b is expressed as a percent ratio of a beam deflection displacement at the beam clevis to the beam length 1600mm (in Figure 2.4). Yielding points of beam longitudinal bars and beam PC tendons are shown by squares and solid circles respectively. The maximum points of beam shear forces are shown by solid diamonds. Hysteresis characteristics had the tendency to exhibit an origin-oriented shape as λ is close to 1.0 gradually. Since the only difference was whether grout was injected into the sheath tube or not, when specimens GB-2 and SB-3 were compared with specimen UB-1, the hysteresis characteristic was influenced by the bond condition along a PC tendon. Beam PC tendons with twisted rib were ruptured after peak beam shear forces for specimens N-4, N-5, M-2, M-5 and GBS-4.

3.2. Bond along PC tendon in a Beam-Column Joint

Tensile force distribution along a PC tendon for specimen GB-2 is shown in Figure 3.2 at each peak R_b . Strain gauges along a PC tendon within a joint panel were attached at two points (denoted as the point (a) and the point (b)) as illustrated in Figure 3.3. The distance was 110mm between these points. Bond stress along a PC tendon in a beam-column joint (denoted as τ_{jp}) was expressed as follows,

$$\tau_{jp} = \frac{T_a - T_b}{110 \cdot L_D} \quad (3.1)$$

where T_a , T_b : tensile force at the point (a) and (b) respectively, and L_D : nominal perimeter of a PC tendon.



Photograph 2.1 Loading apparatus

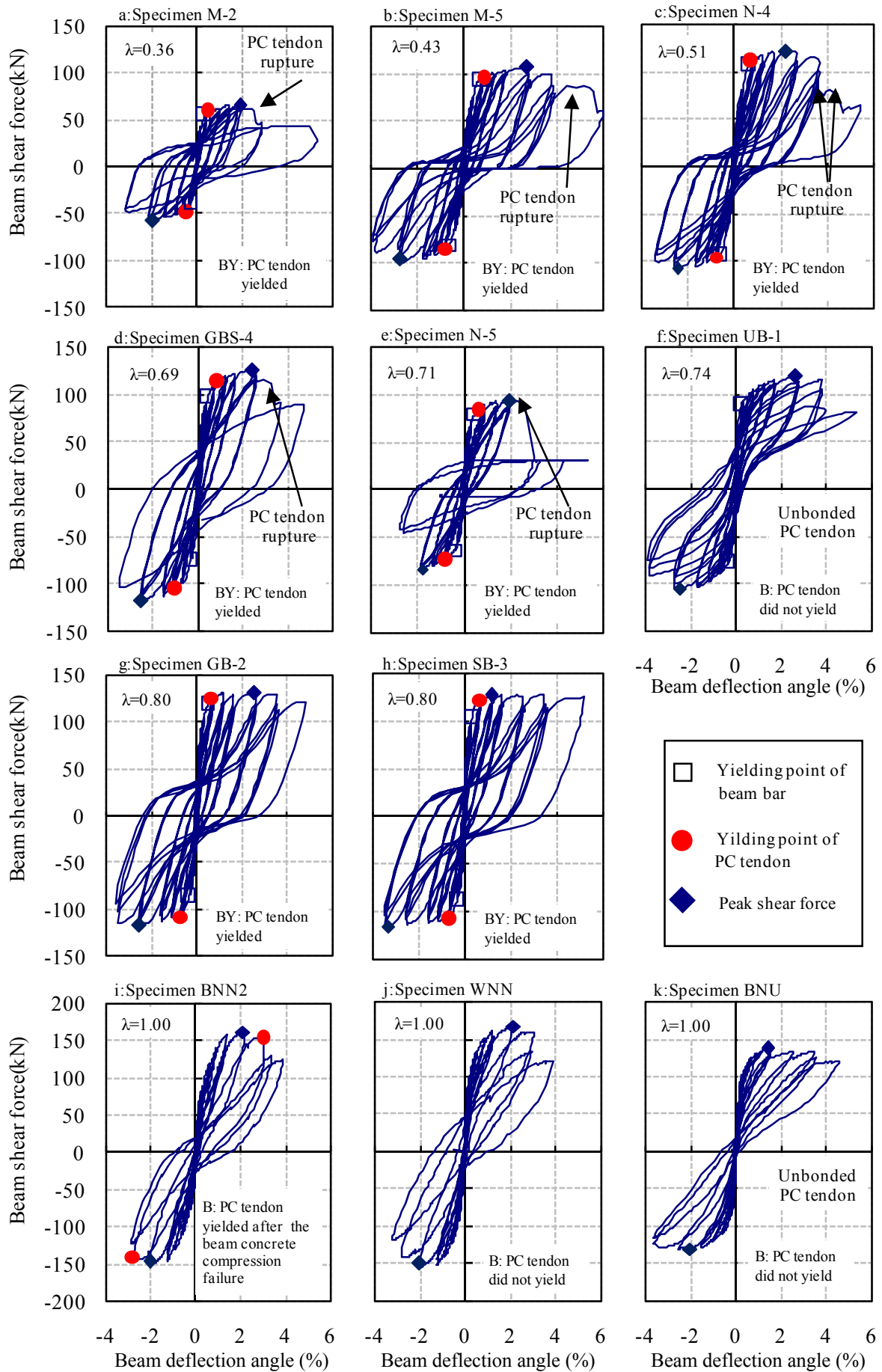


Figure 3.1 Beam shear force-Beam deflection angle relations

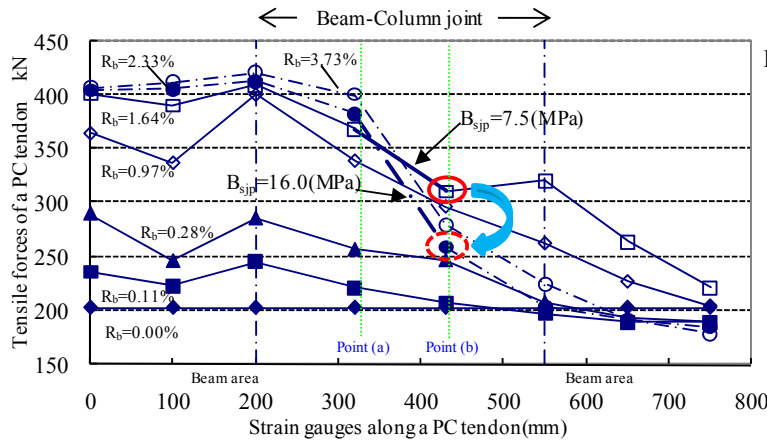


Figure 3.2 Tensile force distributions of PC tendon

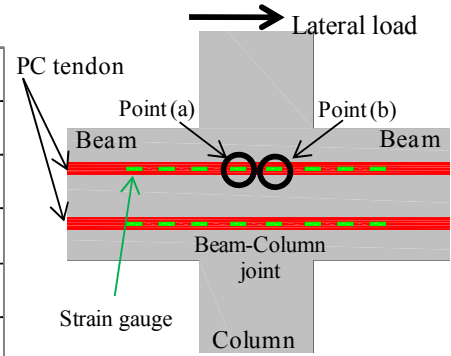


Figure 3.3 Locations of strain gauge

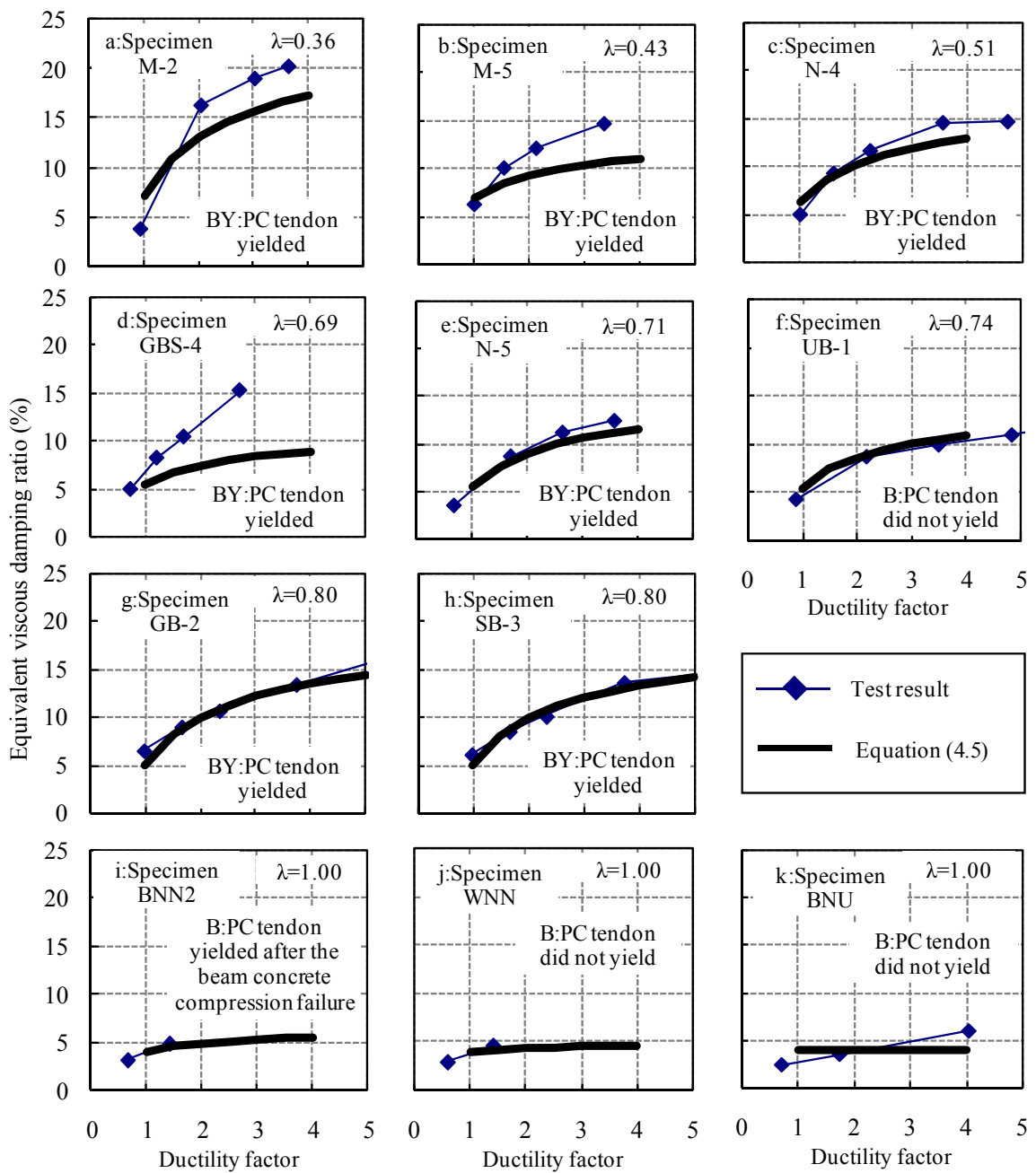


Figure 3.4 Equivalent viscous damping ratio-Ductility factor relations

Table 3.1 Properties of bond index and bond condition observed in tests

	N-4	N-5	M-2	M-5	UB-1	GB-2	SB-3	GBS-4	BNN2	WNN	BNU
B_l	0.69	0.53	0.58	0.86	0.47	0.47	0.47	0.75			
B_{lpt}	1.17	1.18	0.92	1.51		0.63	0.63	1.49	1.45	1.63	
Bond Condition along a PC tendon in test results	Poor bond		not measured	Poor bond		good bond	good bond	not measured	Poor bond	not measured	
σ_{py} (MPa)	1350		1375	1420	1042			1420	1014	1795	1014
σ_{pt} (MPa)	741	676	833	768	557	536	536	720	290	1001	573
$d_{b,pt}$ (mm)	10.7		9.2	12.6	22			12.6	32	12.4	32
D_c (mm)	350										
σ_0 (MPa)	7.59										
σ_G (MPa)	56.4					65.3			54.0		

σ_{py} : yield strength of PC tendon, σ_{pt} : effective prestressing stress, $d_{b,pt}$: nominal diameter of PC tendon

D_c : depth of column, σ_0 : column axial stress, σ_G : grout compressive strength

As the R_b increased from 1.6% to 2.3%, the tensile force at the point (b) decreased (from enclosed solid line to enclosed dotted line in Figure 3.2). Bond stress τ_{jp} increased from 7.5MPa to 16.0MPa as a result. This increase in the bond stress at a middle joint region was caused by the decrease in a tensile force of a PC tendon at the point (b) due to bond action along the PC tendon transmitted well from surrounding concrete compressed by bending moment at the beam end. For specimen SB-3, this situation was the same. The deformed prestressing bar had good bond performance. It was judged for all specimens whether a bond condition along a PC tendon within a beam-column joint was good or poor from such a change of the bond stress τ_{jp} . Bond conditions along a PC tendon in a beam-column joint observed in the tests are summarized in table3.1, which is discussed later.

3.3. Equivalent viscous damping ratio

A beam equivalent viscous damping ratio-ductility factor relations are shown in Figure3.4 by solid diamonds in order of λ . Solid lines computed by the proposed equation (4.5) are discussed later. The yield deflection for a beam to compute a ductility factor was adopted as the yielding point of a PC tendon. There was, however, no obvious point where the stiffness changed suddenly in a beam force – deflection relation for specimens without yielding of PC tendons, denoted by B in Table 2.1. Then the yield deflection for such specimens was defined as the point where the tangent stiffness reduced to 6 % the initial elastic stiffness. An equivalent viscous damping ratio was computed for a loop during a second loading cycle with the same peak R_b as a first loading cycle in beam shear force- beam deflection angle relations. It is recognized qualitatively that energy dissipating ability decreased with the increase in λ . An equivalent viscous damping ratio h_{eq} is discussed in details later.

4. PROPOSED EQUATION AND SENSITIVITY ANALYSIS

4.1. Bond Index for a PC Tendon

Bond failure interfaces around a PC tendon exist probably in following three layers; between concrete and the surface of a sheath tube, between the inside of a sheath tube and grout mortar and between the inside of grout mortar and the surface of a PC tendon. In this paper bond failure interface only between the inside of grout mortar and the surface of a PC tendon was taken into account on the basis of past test results in references [Sanada A.] and [Miyazaki H.] as illustrated in Figure 4.1. A bond index for a PC tendon within a PRC and PC joint panel (denoted as B_{lpt}) is proposed following the equation (1.2);

$$B_{lpt} = \frac{u_{b,av,pt}}{\tau_{u,pt}} \quad (4.1)$$

where the $u_{b,av,pt}$ indicates an average bond stress along a PC tendon within a PRC and PC joint panel when beam PC tendons have tensile yield stress at a beam critical section and keep effective prestressing stress at the opposite beam critical section. This bond stress $u_{b,av,pt}$ is expressed as follows;

$$u_{b,av,pt} = \frac{(\sigma_{py} - \sigma_{pi}) \cdot d_{b,pt}}{4D_c} \quad (4.2)$$

where σ_{py} : yield strength of the PC tendon, σ_{pi} : effective prestressing stress in the PC tendon, $d_{b,pt}$: nominal diameter of the PC tendon and D_c : column depth.

The $\tau_{u,pt}$ indicates the bond strength along a beam PC tendon passing through a PRC and PC joint panel, which is expressed as follows;

$$\text{if the PC tendon is a deformed bar; } \tau_{u,pt1} = 0.7 \left(1 + \frac{\sigma_0}{\sigma_G} \right) \sigma_G^{2/3} \quad (4.3)$$

$$\text{if the PC tendon is a strand or a deformed bar with twisted ribs; } \tau_{u,pt2} = \frac{1}{3} \cdot \tau_{u,pt1} \quad (4.4)$$

where σ_0 : column axial stress and σ_G : compressive strength for grout mortar.

Equation (4.3) followed the equation (1.4) for a deformed bar. Past test results of pulling a PC tendon out of a concrete cube [Miyazaki H.] is shown in Figure 4.2. It is appropriate in this paper to regard the first peak bond stress in Figure 4.2 as the bond strength for a PC tendon with twisted ribs because a slip of a PC tendon within a beam-column joint is usually small. A prestressing strand and a prestressing deformed bar with twisted ribs had equal bond performance when references [Sanada A.], [Miyazaki H.] and [Korenaga T.] are compared. Since the first peak bond stress for a deformed bar with twisted ribs was one-third that for a deformed bar in Figure 4.1, the equation (4.4) is expressed as one-third of the equation (4.3). Bond index B_{lpt} greater than unity represents poor bond condition along a PC tendon within a joint panel, and that equal to or less than unity does good bond condition. Two bond indices for a beam bar and a PC tendon in a joint panel computed by the equations (1.2) and (4.1) respectively, the bond conditions along a PC tendon observed in the tests, and values used to compute these bond indices are summarized in Table 3.1. Although there were a few specimens where tensile forces along a PC tendon within a joint panel were not able to be measured, the index B_{lpt} was useful to classify well the bond conditions along a PC tendon in test results.

4.2. Proposed Estimation of Equivalent Viscous Damping Ratio

The equation (4.5) to estimate an equivalent viscous damping ratio h_{eq} for a flexural beam in a PRC frame is proposed as follows;

$$h_{eq} = 0.04 + 0.05(1 - \lambda) + \left(\frac{0.1(1 - \lambda)}{B_l^2} + \frac{0.1 \cdot c \cdot \lambda}{B_{lpt}^2} \right) \left(1 - \frac{1}{\sqrt{\mu}} \right) \quad (4.5)$$

where B_l is a same index as the equation (1.2) and B_{lpt} is obtained by the equation (4.1). Coefficient of $\frac{0.1 \cdot c \cdot C_{pcr}}{B_{lpt}^2}$ c was chosen to be 0.4 to fit test results. If unbonded PC tendons are used, the term of $\frac{0.1 \cdot c \cdot C_{pcr}}{B_{lpt}^2}$ is omitted because it is impossible to define the B_{lpt} index. For RC structures ($\lambda = 0$), the h_{eq} becomes a constant value of 0.09 in the equation (1.1) when the ductility factor μ is equal to 1.0. For PRC and PC

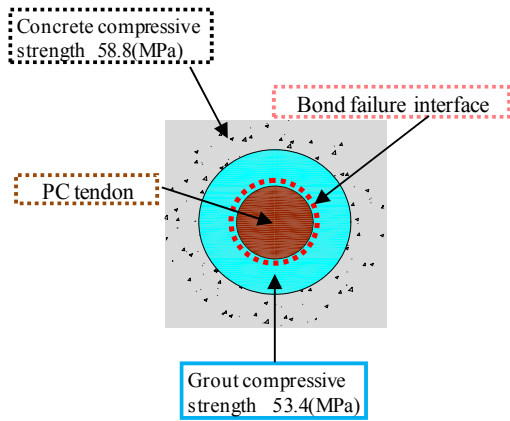


Figure 4.1 Bond failure interface

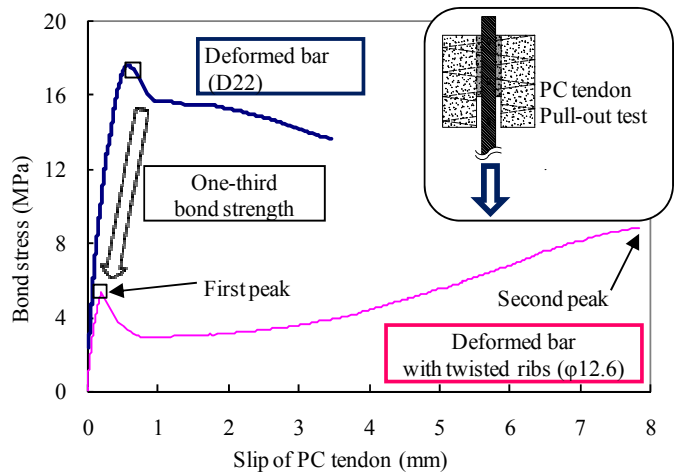


Figure 4.2 Past pull-out test result

structures, the constant term at $\mu=1$ in the equation (4.5) was determined to be $(0.09-0.05\lambda)$ by a regression analysis based on the least squares method. For specimens M-5 and GBS-4, an equivalent viscous damping ratio predicted by the equation (4.5) was larger than that obtained by the tests. It is necessary to investigate in details the reason why the prediction by the equation overestimated test results. Except for specimens M-5 and GBS-4, the h_{eq} predicted by the equation for a PRC flexural beam within interior beam-column subassemblages agreed well with that obtained by laboratory tests.

4.3.Sensitivity Analysis

Results taken from sensitivity analyses for the proposed equation (4.5) are shown in Figures 4.3 and 4.4. A prestressing ratio of 1.0, 0.8, 0.5 and 0.3 was chosen as a respective parameter in Figure 4.3. The bond index B_l of 0.6 and 2.0 represents a very good and very poor bond condition respectively along a beam bar. The bond index B_{lpt} of 0.6 and 3.0 represents a very good and very poor bond condition respectively along a PC tendon. The combination of B_l and B_{lpt} is shown by four lines in Figure 4.3. Solid lines indicate a very good bond condition along both a beam deformed bar and a PC tendon in a joint panel. It is found that an equivalent viscous damping ratio increased and PC tendon bond contribution to an equivalent viscous damping ratio decreased as λ decreased from 1.0 to 0. An equivalent viscous damping ratio- λ relation and contribution ratio to an equivalent viscous damping ratio- λ relation are shown in Figure 4.4 (a) and (b) respectively when ductility factor is 4 and the both bond indices B_l and B_{lpt} are 0.6. An equivalent viscous damping ratio- λ relation and contribution ratio to an equivalent viscous damping ratio- λ relation are shown in Figure 4.4 (c) and (d) respectively when ductility factor is 4 and the bond indices B_l and B_{lpt} are 1.0 and 0.6 respectively. When a prestressing ratio λ was equal to 0.71 in Figure 4.4(b) and 0.47 in Figure 4.4(d), a contribution of bond condition along a PC tendon to the total of the h_{eq} value became even with that along a beam bar. When λ is 1.0, a contribution ratio of a good bond along a PC tendon passing through a beam-column joint was 58.2%. When a prestressing ratio λ is greater than 0.5, a good bond condition along a PC tendon gave a remarkable influence on the energy dissipation ability.

5. CONCLUSIONS

The following conclusions can be drawn from the present study:

- (1) An equivalent viscous damping ratio predicted by the proposed equation for a PRC flexural beam interior beam-column subassemblages agreed well with that obtained by laboratory tests.
- (2) The bond index for a PC tendon in a beam-column joint computed by the proposed equation was able to predict the bond condition along a PC tendon observed in the tests.
- (3) When a prestressing ratio λ is greater than 0.5, a good bond condition along a PC tendon gave a remarkable influence on the energy dissipation ability.

REFERENCES

- Kishida S., Kitayama K., Maruta M., Moriyama K. (2004). Earthquake Resistant Performance and Failure Mechanism of Precast Prestressed Concrete Beam-Column Joints Assembled by Post-Tensioning Steel Bars. Proceedings, 13th World Conference on Earthquake Engineering, **CD-Rom**, No.1763
- Kitayama K., Tajima Y., Kishida S., Miyazaki H. (2006). Restoring Force Characteristics of Prestressed Reinforced Concrete Interior Beam-Column Subassemblages Focusing on Bond Performance along Beam Bars (Part 1 and Part 2). *Summaries of Technical Papers of Annual Meeting of Architectural Institute of Japan*-2,1-4.
- Kitayama K., Tajima Y., Yajima R. (2008). Evaluation of Earthquake Resistant Performance for Prestressed Reinforced Concrete Interior Beam-Column Subassemblages(Part1-3). *Summaries of Technical Papers of Annual Meeting of Architectural Institute of Japan*-2,157-162.
- Architectural Institute of Japan.(2004). Guidelines for Performance Evaluation of Earthquake Resistant Reinforced Concrete Buildings (Draft).
- Sanada A., Maruta M. (2003). Bond Strength under Several Combination of Prestressing Steel and Grout Materials. *Summaries of Technical Papers of Annual Meeting of Architectural Institute of Japan*-2,571-572.

Miyazaki H., Kitayama K., Tajima Y. (2007). Bond Strength along PC Tendon within Sheath by Pull-out Test. *Summaries of Technical Papers of Annual Meeting of Architectural Institute of Japan*-2, 141-142.
 Korenaga T., Watanabe H. (1999). Model of the Bond Characteristics between Prestressing Strand and grout mortar. *Summaries of Technical Papers of Annual Meeting of Architectural Institute of Japan*-2, 1083-1084.

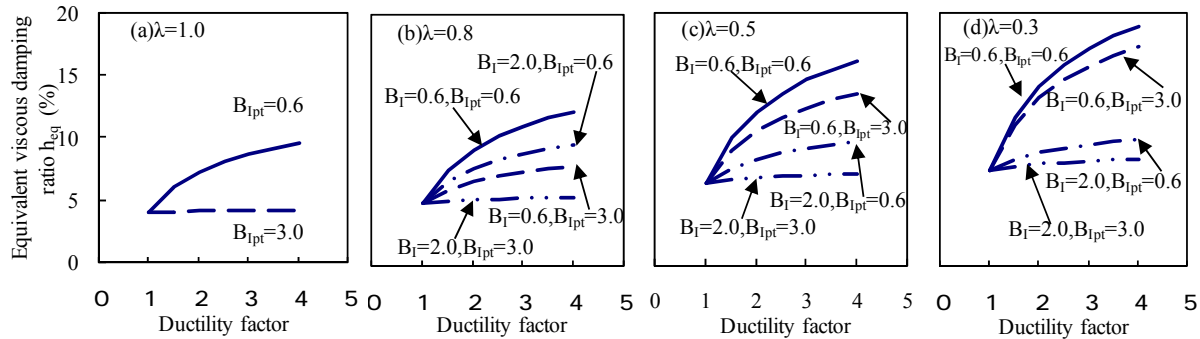


Figure 4.3 Equivalent viscous damping ratio-Ductility factor relationships

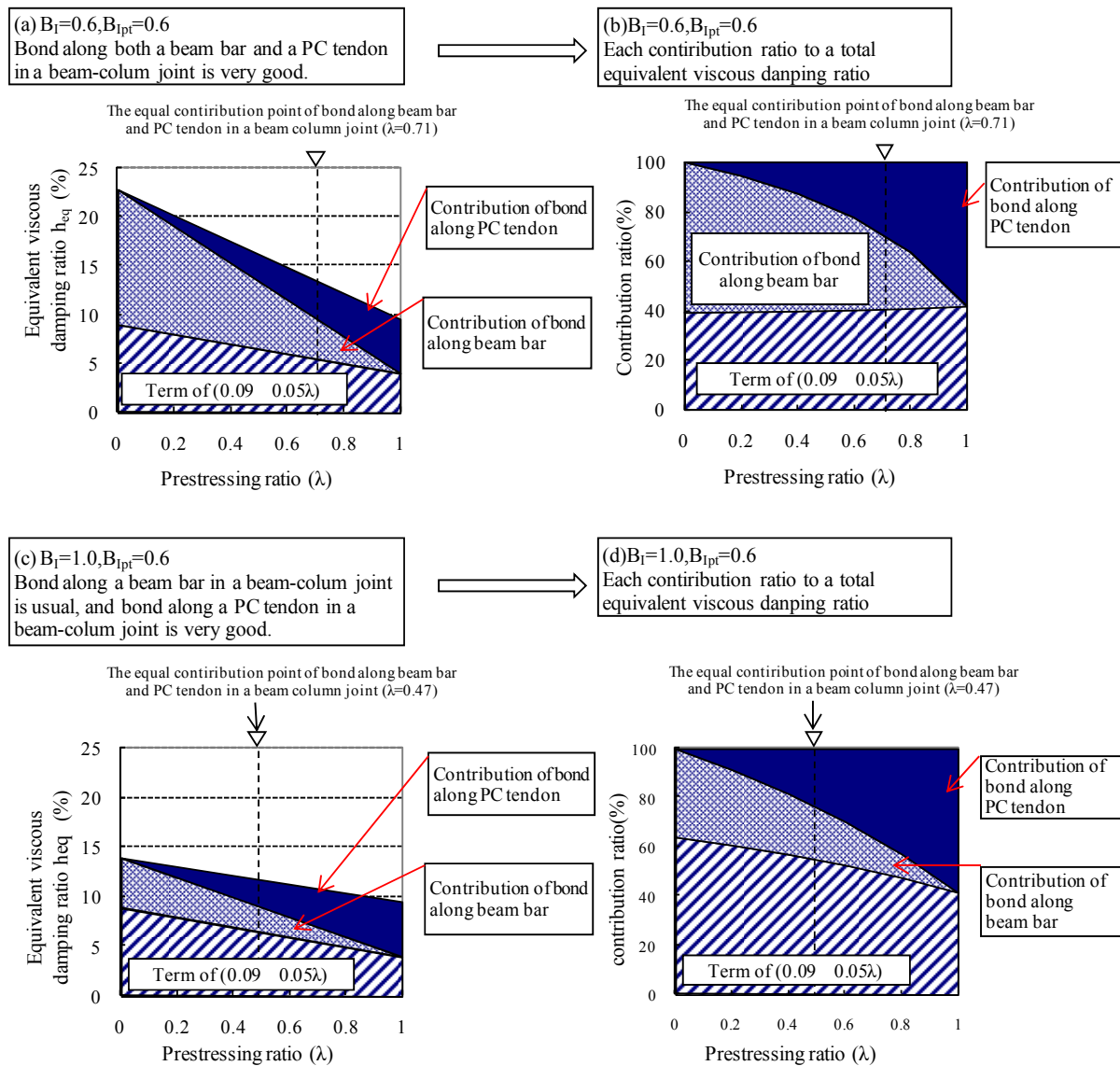


Figure 4.4 Equivalent viscous damping ratio-Prestressing ratio relationships (Ductility factor is 4)